

Suppressing fluid loss in fractures

Boaz van der Plas · Michael Golombok

Received: 21 August 2014 / Accepted: 2 February 2015 / Published online: 14 February 2015
© The Author(s) 2015. This article is published with open access at Springerlink.com

Abstract Injected fluid losses in large subsurface channels can be suppressed with the use of low concentrations of viscoelastic surfactants which selectively retard flow in larger apertures. The effect is demonstrated by pumping viscoelastic surfactants through smooth capillaries. The choice of capillary diameters relate to fractures in oil or geothermal reservoirs as well as induced hydraulic fracturing operations in tight gas reservoirs. Selective retardation is favoured at a lower range pressure drops usually associated with oil recovery. The effective apparent viscosity contrasts between different capillary diameters are not as high as those previously observed in permeable flow because the measured effects in the smooth capillaries are mainly shear driven. We expect an elongation contribution to the apparent viscosity in real non-smooth fractures.

Keywords Hydraulic fracturing · Geothermal · Secondary oil recovery · Fracture flow · Viscoelastic surfactants

List of symbols

A Cross-sectional area
d Diameter
h Height
K Permeability
 L_m Lateral extent of matrix

p Pressure
Q Flow
 v Mean velocity
x Flow direction
w Width

Greek

α Viscosity rate
 γ Shear rate
 Λ Total resistance to flow
 μ Shear viscosity from rheometer
 μ_{app} Apparent viscosity from capillary
 ρ Density

Subscripts

0 Base fluid
a Additive
eff Effective
f Fracture
l Large
m Matrix
s Small

Introduction

Controlling fluid flow in channels and fractures is important in three different aspects of energy recovery from the subsurface:

- During the initial stages of hydraulic fracturing, the pressurised injected water “pad” needs to be selectively stopped from entering large fractures. This enables more volume to be directed into small fractures where more surface area needs to be created to enhance fracture conductivity.

B. van der Plas (✉) · M. Golombok
Faculty of Mechanical Engineering, Technische Universiteit
Eindhoven, Den Dolech 2, 5600 MB Eindhoven,
The Netherlands
e-mail: b.plas@tue.nl

B. van der Plas · M. Golombok
Shell Global Solutions International B.V., Kessler Park 1,
2288 GS Rijswijk, The Netherlands

- In enhanced geothermal systems in granite basement, injected water is diverted via larger fractures. The diverted water is not heated and cools down the other hot streams from smaller fractures when they are combined at the producer well. These “short circuits” are thus limiting factors on efficient high quality heat recovery.
- In secondary oil recovery, uneven advance of the displacing injected fluid arises from “short circuits” caused by large fractures diverting water around, and thereby bypassing, oil bearing zones.

The first two cases refer to competing fractures (Fig. 1a) and the third case to fractures diverting injected fluid from the porous matrix (Fig. 1b).

Recent research (Golombok et al. 2008; Reuvers and Golombok 2009a, b; Golombok and van der Wijst 2012) has demonstrated the potential of viscoelastic surfactants (VES) in selectively retarding flow in regions of high rock permeability for application in oil recovery. So far these VES materials have not been studied in the other source of oil bypass i.e., fracture flow. This is the subject of the current paper.

Viscosity modifying additives are generally characterized by their response to changing shear in a standardised situation such as a Couette cell. The viscosity is mapped for a range of shear rates measured one at a time. Couette cell measurements with their constant applied shear rate do not extrapolate straight-forwardly to direct application in an idealized capillary or slit flow. In porous and aperture (fracture, capillary etc.) flow there is a distribution of shear rates within the openings. The apparent viscosity is different from measurements in Couette cells. A study of viscosity modifying additives in fractures, slits and

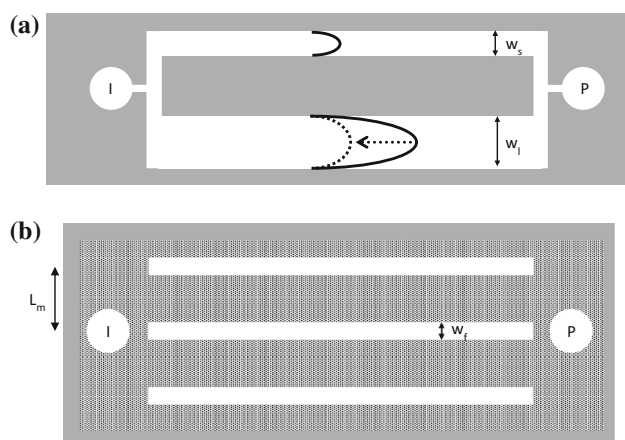


Fig. 1 Subsurface fluid loss fracture (a) dual fracture system in impermeable rock. Selective retardation in larger fracture indicated by dotted line (b) fracture in permeable rock. *I* and *P* represent the injector and producer, respectively. The height of the fractures is perpendicular to the plane of the drawing

capillaries is a logical intermediate step between Couette cells and porous media. Slits and capillaries have a well-defined geometry where the behaviour of fluid flow is simpler than for porous flow. Demonstrating selective retardation in capillaries is the focus of this paper i.e., the link between effects observed in Couette cells and in porous media. “Background” describes the physical processes and connects these with the application. An experimental description follows in “Experiment” and the results are analysed and discussed in “Results and discussions”.

Background

Fracture/fracture flow

Figure 1a shows a schematic subsurface system with two different sized rectangular channels with width w_l (large) and w_s (small). (The height h is always much greater than the fracture width.) The fractures are parallel in the system and thus an equal pressure drop exists over both fractures. This is applicable to both the geothermal and hydraulic fracturing scenarios mentioned above. The mean velocity for a Newtonian fluid such as water or brine is described by Turcott and Schubert (1982)

$$v = \frac{w^2 \Delta p}{12\mu \Delta x} \quad (1)$$

which is very similar to the form for flow in a capillary of diameter d used in the experiments described later.

$$v = \frac{d^2 \Delta p}{32\mu \Delta x} \quad (2)$$

In terms of flow rate between a large (l) and small (s) capillary, the relative velocities and flow rates are determined by $(d_l/d_s)^2$ and $(d_l/d_s)^4$, respectively. Fluid is thus easily diverted via a large fracture/capillary. To solve this “short circuit” problem, the fluid velocity in the large fracture has to slow down—as is indicated with the dashed line in Fig. 1—while the fluid velocity in the small fracture and injector remains the same (Dogon and Golombok 2014).

Suppose now that the viscosity of the fluid can be chosen separately in two different capillaries such that the mean velocity in the fractures becomes equal. This is achieved when the viscosity ratio is

$$\frac{\mu_l}{\mu_s} = \left(\frac{w_l}{w_s}\right)^2 \quad (3)$$

with a cubic dependence if we wish to equalise flow rate as in the first example. The shear rate is the parameter which determines the effective viscosity. The wall shear rate increases with aperture size. It decreases to zero at the centre—linearly for a Newtonian fluid. A non-Newtonian fluid

showing shear thickening thus seems to be a good candidate to obtain selective fluid retardation in large fractures. However, the injection well has the largest dimensions in the system and the fluid will become highly viscous there making injection difficult. Viscoelastic surfactants have the potential to overcome these problems. Before examining these we summarise the case of competitive fracture/matrix flow.

Fracture/matrix flow

The case of fracture diversion away from permeable porous flow is more difficult because of the much greater contrasting effective permeabilities. For example, if two competing fractures (Fig. 1a) have a width ratio w_f/w_s of 10, the ratio of permeabilities is 100. For fracture and matrix (Fig. 1b), the effective permeability ratio is higher—this can be as much (see “Appendix”) as 10^5 . Fractured oil fields typically have dual porosity structure derived from porous matrix and fractures, respectively (van Golf-Racht 1982). Intergranular porosity is associated with primary matrix permeability K_m . Secondary porosity arises from fractures and has an secondary (intrinsic) fracture permeability K_f defined by Eq. (1). (Occasionally one sees references to an effective (conventional) fracture permeability which is a spatial average over a matrix block containing a fracture—see “Appendix”)

The main concern of course is the vast volume of fluid which is lost via the “short circuit” resulting from fractures diverting fluid. The fractional pumped fluid loss to the fracture (Fig. 1b) is given by

$$f = \frac{Q_f}{Q_m + Q_f} = \frac{1}{(K_m L_m / K_f w_f) + 1} \quad (4)$$

for the case of a Newtonian fluid where L_m is the lateral extent of matrix which typically defines the fracture periodicity. We want to reduce this fluid loss by impeding entrance to fracture flow so that the injected water rather directly penetrates the matrix. In the preceding section we postulated different viscosities for different fracture sizes. We now analogously do this for the fluid between matrix (viscosity μ_m) and fracture (viscosity μ_f) in Fig. 1b. The flow rate ratio now becomes

$$\frac{Q_m}{Q_f} = \frac{L_m K_m \mu_f}{w_f K_f \mu_m} \quad (5)$$

Typical values of L_m are 10–50 m with an emphasis on the lower end of the range for limestones and larger grained sandstones. For permeabilities, typical permeability values recently cited by van Heel et al. (2008) are $K_m = 10$ mD and $K_f = 500$ D corresponding to a value of $w_f \sim 100 \mu\text{m}$. In that case, the fractional fluid loss to the fracture is ca. 30 %. Viscosity contrast ratios of 10 have been previously

demonstrated in viscoelastic surfactant solutions in permeable flow and in this case would reduce the diversion from 30 % to around 5 %.

Viscoelastic surfactants

The novel rheology is displayed in a solution with low concentrations of two chemicals: a surfactant CTAB and a co-solute NaSal in base fluid (Hartmann and Cressely 1998). Together these additives create a viscoelastic solution with a non-monotonic viscosity shear rate response, i.e., the fluid can behave as shear thinner and shear thickener depending on the shear range. Rojas et al. (2008a, b, 2010) showed that the apparent viscosity in porous media is higher than for “simple” shear flow in a rheometer. Rojas assumed that the extensional shear in porous media is entirely responsible for increase in apparent viscosity. Gonzales et al. (2005) and Rojas et al. (2008a, b, 2010) introduced an expression for the total resistance to flow in structured porous media:

$$\Lambda = \frac{K_{st} \Delta p}{\mu_0 v \Delta x} \quad (6)$$

Here K_{st} denotes the structure determined permeability and the base solvent viscosity (i.e. water). The dimensionless resistance factor (Λ) is then proportional to the apparent viscosity

$$\mu_{app} = \Lambda \mu_0 \quad (7)$$

Golombok et al. (2008) used this formalism to show that these additives can result in selective fluid retardation for permeable flow in porous materials such as reservoir rocks. The resistance to flow (the effective viscosity) responds to the local permeability.

The rheology of VES fluids has also been studied in a number of flow configurations. Cheung et al. (2012) studied CTAB/NaSal solution through a microfluidic device containing an array of microposts (100 μm diameter, 10 μm apart). Yamamoto et al. (2008) described a 30/60 mM CTAB/NaSal solution flowing through a capillary with a diameter of 4.3 mm. This study focussed on the shear rate jump—the region where the shears stress is independent of the shear rate. The only pressure-driven flow study of VES solutions was through an array of cylinders by Moss and Rothstein (Moss and Rothstein 2010). Selective retardation has been demonstrated in permeable flow in a porous medium but not to our knowledge in aperture/capillary flow.

Experiment

A schematic overview of the experimental setup is given in Fig. 2. The injection fluid in the intake container (1) is

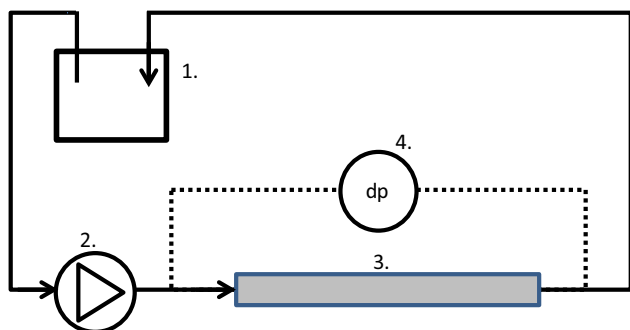


Fig. 2 Experimental setup. 1 injection fluid in intake container (2) Quizix QX6000 dual syringe pump (3) capillary, (4) differential pressure transducer

pumped by a Quizix QX6000 dual syringe pump (2) through a capillary (3) The flow rate of the injected fluid is measured at the pump outlet and the pressure drop over the capillaries is measured by a Rosemount –460–460 mbar and a Rosemount –20–20 bar differential pressure transducer (4) with connections to the upstream and downstream side of the capillary.

We used capillaries with inner diameters 0.25 and 0.60 mm, respectively. This size was chosen to reflect the applications as outlined in the introduction, and represents an intermediate value between the fracture short circuit oil recovery regime (ca. 100 μm) on one hand (van Heel et al., 2008) as in “Fracture/matrix flow” above, and the geothermal and hydraulic fracturing (Turcott and Schubert 1982) (ca. 1 mm) on the other. The capillaries are made of stainless steel and glued in flexible polyurethane tubing to prevent bending and for easy installation in the experiment. The CTAB and NaSal were dissolved in deionised water. We denote the concentrations as $[\text{CTAB}]/[\text{NaSal}]$ where $[\text{CTAB}]$ and $[\text{NaSal}]$ are the concentrations CTAB and NaSal in milli-moles/l. A representative brine was 3 wt % NaCl (roughly seawater).

After placing the capillary in the setup, water is injected. Having flushed the system, the bypass of the core flooding system is opened and the pressure transducer piping is deaired by opening the valves on top of the pressure transducer. After this step, all the air in the system is removed and the bypass valve is closed. The setup is now ready for measurement.

Results and discussion

Although some experimental work has previously shown the classical behaviour as discussed in “Fracture/matrix flow”, the majority of solutions show the rheometric response shown in Fig. 3, where we have compared 5/5 mM VES solution in water and brine. The non-monotonic

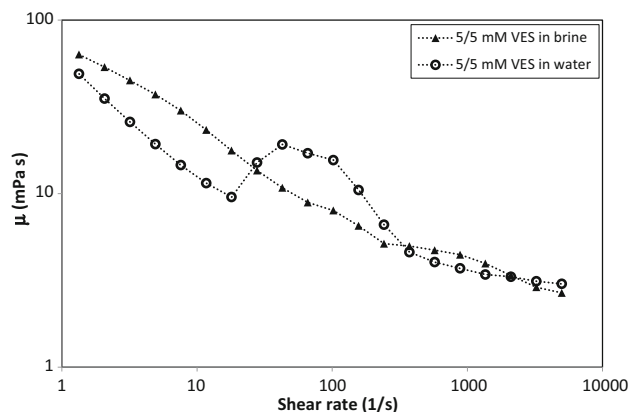


Fig. 3 Rheometer shear rate—viscosity response of 5/5 mM VES in water and in brine

behaviour between 10 and 100 s^{-1} is effectively removed by the addition of salt.

A different concentration and concentration ratio of VES solution is demonstrated in Fig. 4. Both solutions (N. B 7.5/5 mM and 5/5 mM solution in water) have comparable behaviour over the shear thickening and thinning regime—the main difference is that the equimolar solutions also demonstrate an additional shear thinning effect between the zero shear viscosity and the critical shear rate (i.e., the subsequent onset of thickening). Later we shall show that such initial shear thinning does not exclude selective retardation of flow in larger apertures. One question in this respect is whether the existence of the “hump” (i.e., region of thickening followed by thinning) is required to see retardation effects in channels or capillaries.

In contrast to the above described rheometer measurements, a pressure driven flow in a capillary has no unique shear associated with a particular pressure drop and flow rate. The shear rate (for Newtonian fluids) at any point within the capillary is proportional to the radial distance from the centre. It varies from 0 at the centre line to a maximum value at the wall. In a 0.25 mm capillary, the smallest mean velocity reproducibly achievable was 44 mm/s. This means that the range of shear rates in the flow extends from 0 s^{-1} at the centre to 128 s^{-1} at the wall for water. In Figs. 3 and 4 the region of shear thickening and thinning encompasses 20–200 s^{-1} , so we may expect a radially varying viscosity across the capillary. Similar arguments apply to the 0.6 mm capillary where the smallest achievable velocity was 17 mm/s. The shear thus varies between 0 and 227 s^{-1} and thus also encompasses part of the shear thickening and thinning region of the curves in Figs. 3 and 4. The net flow is determined by the range of shear rates convoluted with the rheometer viscous response shown in Figs. 3 and 4.

An apparent difficulty with this analysis is that we have used water estimates and then applied Couette responses of

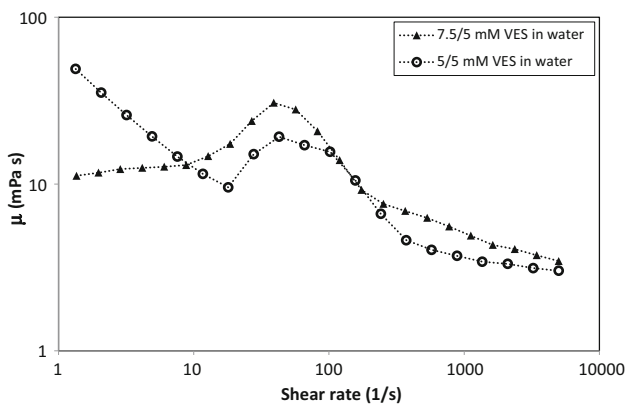


Fig. 4 Rheometer shear rate—viscosity response of 5/5 mM VES and 7.5/5 mM VES in water

VES solutions. VES fluids are non-Newtonian and because of the complex behaviour it is not straightforward to calculate the wall shear rate in a capillary. However, a previous study (Yamamoto et al. 2008) suggests a plug flow profile for VES fluids which means a rapid shear rate decay near the wall. Therefore the maximal shear rates at the wall for VES solutions are expected to be higher than for water. Thus, we expect that the shear rate range at least includes that from 0 to 128 s⁻¹. These shear rates overlap the shear rates (measured with the Couette cell) associated with the non-monotonic range of Figs. 3 and 4, although we will later show that this is not absolutely necessary for selective retardation in capillaries.

As explained above, the Couette cell applies a single shear rate whereas in a capillary there is a range of shear rates. The non-Newtonian VES solutions thus give different shear distributions in capillaries of different dimensions which result in different apparent viscosities. This is what causes the selective retardation in one of the capillaries. For our application the object is to have selective retardation in the larger aperture capillaries or fractures. This has been previously demonstrated (Golombok and van der Wijst 2012) in materials of contrasting matrix permeability: for a high permeability of 2200 mD and a low permeability of 45 mD, the water velocity ratio is 49 times whereas with low equimolar concentrations of VES (1.5 mM) it is reduced to 10.

Figure 5 compares the VES response in 0.25 mm and 0.6 mm diameter capillaries over a range of identical pressure drops for a 7.5/5 mM solution in water. The corresponding lines for water are shown for reference. In the 0.25 mm capillary the velocity/pressure drop curve is linear. The velocity is reduced to ca. 25 % of its water value. In the 0.6 mm capillary however, the velocity–pressure curve is non-linear with velocity retardations in the range 10–33 %. We define the retardation by

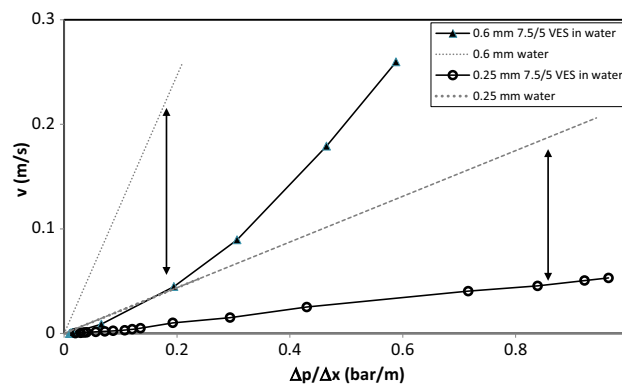


Fig. 5 Comparison of 7.5/5 mM VES with water in 0.25 mm and 0.6 mm capillaries. The broken lines show the water response and the solid lines show the VES response. The arrows link water and VES response for the same capillaries

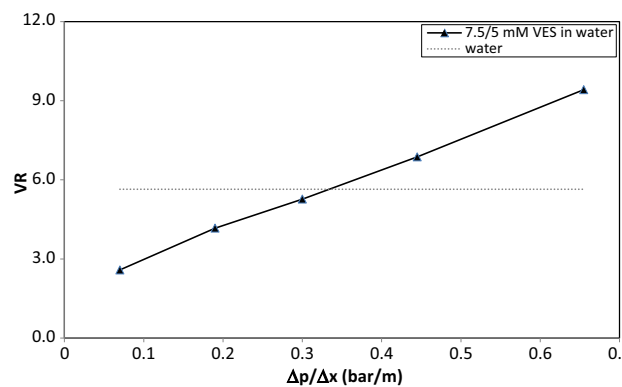


Fig. 6 Velocity ratio for two capillaries with 7.5/5 mM VES (VR_a in text) compared to water (VR_0 in text). $VR_a < VR_0$ is the region where selective retardation occurs in the larger capillary

$$VR = \left(\frac{v_l}{v_s} \right) \Delta p / \Delta x \tag{8}$$

where l and s refer to large and small capillaries. VR_0 refers to the base fluid case (water or brine) and VR_a refers to the case when a viscoelastic surfactant combination additive is present. This is plotted as a function of the pressure drop gradient in Fig. 6. VR_0 is shown as a reference. This is of course constant—it is purely dependent on the capillary diameters and does not vary with pressure gradient. VR_a does of course vary. When $VR_a < VR_0$ then the flow in the larger capillary has been selectively retarded due to the higher viscosity. When $VR_a > VR_0$, the effect is reversed. The cross over point for the solution in Fig. 6 is around 0.3 bar/m. The effect is of course dependent on the solution concentrations used. It does however indicate that selective retardation is possible at a range of lower pressure drops—in fact those associated with far field mid-reservoir locations far from the well bore—and is related to the induced changes in apparent viscosity.

The apparent viscosity for the 5/5 mM VES in brine is obtained following the procedure previously used (Rojas et al. 2008a, 2008b, 2010) for permeable flow and based on Eq. (6) above. These different apparent viscosities are shown for the two capillaries in Fig. 7. The viscosities in the large capillary are higher at lower pressure drops and the viscosities are basically identical above around 0.5 bar/m. The best viscosity contrast that is obtained is 2.5 times that in the smaller fracture. This is sufficient for reaching a considerable level of retardation but does not halt the flow completely (we would not want to stop flow entirely in a large fracture anyway since these are useful for transporting oil displaced from low permeability matrices).

Comparison with the rheometer response in Fig. 3 for this 5/5 mM VES solution in brine answers two of the questions raised earlier. First of all, despite the lack of a “hump” (i.e., region of shear thickening followed by shear thinning) in the rheometer plot, we still see a selective retardation at lower (and realistic for oil reservoirs) pressure drops as shown by the higher viscosity in the larger (0.6 mm) capillary. Second, we may regard the plot in Fig. 7 as a kind of flow analogue to the Couette plot of Fig. 3. This is a function of the well-known phenomenon that viscosities of non-Newtonian solutions have different values dependent on how they are measured. However, at least for Newtonian fluids, the pressure drop is directly proportional to the shear rate in capillaries and slits. Of course there is a distribution of shear rates moving radially across the capillary and the apparent viscosity reported in Fig. 7 actually represents an average taken across the corresponding plot shown in Fig. 3. We do not actually have any knowledge (or indeed need to know) about the shear rate distribution in the solution in the capillary. The capillary plot in Fig. 7 does not show any non-monotonic “hump” and this correlates with our previous conclusion that selective retardation can be observed even without any shear thickening and then thinning region in the Couette plot.

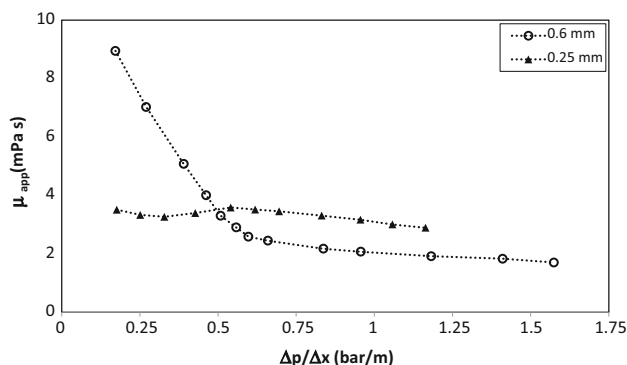


Fig. 7 Apparent viscosity (μ_{app}) of 5/5 mM VES in brine for 0.25 and 0.6 mm capillaries

These effects are also considerably less than the viscosity contrast obtained in permeable flow studies (Golombok and van der Wijst 2012). In that case even for much lower VES equimolar concentrations (1.5 mM) the viscosity contrast was 5 which is two times higher than observed in capillaries in the current studies at considerably higher concentrations (7.5/5 mM). This is due to the nature of the flow. In the capillary we have fully developed flow. However, in permeable flow in a porous medium we have developing flow—or rather, continuously redeveloping flow. The term “developing flow” is normally associated with entrance effects. By contrast, continuously redeveloping flow is what happens inside the porous medium due to the continuous changes in pore geometry and the associated aperture available for fluid flow. This brings in other fluid resistance factors such as extensional viscosity and is the subject of current study.

Using Eq. (6) above, we have been comparing the selective velocity retardation in larger apertures. In the energy recovery systems associated with geothermal and oil, there is a fixed pressure drop between injector and producer so the comparisons need to be made between different sized apertures operating at the same pressure drop. In fact the pressure drop (in the order of 0.1 bar/m for oil recovery and about ten times higher for geothermal systems), is not spread uniformly between injector and producer. Most pressure is lost in the well bore regions leaving only around a quarter of the remaining pressure for driving fluid flow in fractures far from the well bore. This is different for hydraulic fracturing where the flow is also pressure driven but where the constant resistance is provided by the geomechanical strength of rock under confinement by the lithostatic pressure. Figure 5, 6 and 7 have pressure drops relevant to the oil displacement case and show the desired higher capillary flow contrast at lower pressure drops.

These curves do not take into account the reduced velocity in mid-reservoir compared to the near-well bore region. The effects of different pressure drops at varying velocities through the reservoir are assessed by a resistance factor. This is defined by the ratio of pressure drops at identical velocities:

$$RF = \left(\frac{\Delta p_l}{\Delta p_s} \right)_v = \frac{(\mu_{app})_l}{(\mu_{app})_s} \quad (9)$$

This is shown in Fig. 8 which suggests in parallel to the results above, that selective velocity contrasts are obtained below around 0.1 m/s for this particular solution. In oil recovery, typical far field reservoir fluid velocities are in the order of 1 ft/d i.e., 3 $\mu\text{m/s}$. The fracture “short circuits” corresponds to areas of higher “secondary” permeabilities as quantified for an extreme case in “Fracture/matrix flow” above. The resulting velocities will be in the order of 0.1 m/s. This encompasses the velocity range shown in

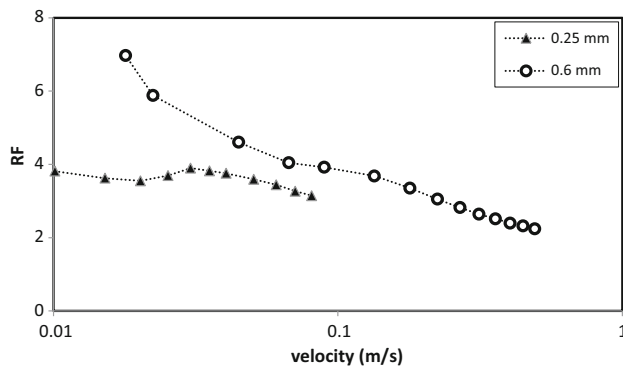


Fig. 8 Resistance Factor (RF) of 5/5 mM VES solution in brine in 0.25 and 0.6 mm capillaries

Fig. 8 although in this example it is right on the border. Further tuning of VES solution compositions is directed at addressing particular ranges of relative primary and secondary (fracture) permeabilities in reservoirs.

Conclusion

1. Low concentrations of viscoelastic surfactant and cosolute in water can selectively retard flow in larger openings of parallel aperture systems. Applications are short circuits in geothermal and oil recovery systems, as well as during hydraulic fracturing.
2. Adding salt removes the non-monotonic effect in a rheometric measurement, however the selective retardation effect is maintained. Such a non-monotonic “hump” is therefore not required for selective retardation in aperture flow (capillaries or fractures).
3. The selective retardation is dependent on the pressure drop and is favoured at the lower values associated with oil recovery. At higher pressures, selective acceleration with respect to water is observed.
4. Viscosity contrasts of up to ten were observed. These were observed up to velocities around 0.1 m/s. Different formulations may yield even larger results.
5. The viscosity contrast is not as high as in permeable flow through porous material. The reason is that in this study the flow is steady state whereas in permeable flow, the flow can be classified as continually redeveloping because of pore geometry variations. Real fractures have continually varying geometries (wall roughness, tortuosity etc.) and are expected to show higher viscosity contrast. This is the subject of further study.

Acknowledgments The authors thank Dr. Gerald Glasbergen and Professor Cor van Kruijsdijk of Shell Global Solutions b. v. for illuminating discussions and pointers.

Open Access This article is distributed under the terms of the Creative Commons Attribution License which permits any use, distribution, and reproduction in any medium, provided the original author(s) and the source are credited.

Appendix

The intrinsic (single) fracture permeability K_f has the fracture void area as the flow cross section of width w_f (Fig. 1b). It is difficult to isolate this value in well tests. What is usually measured is an effective permeability K_{eff} which is derived from a spatial average over a matrix block which contains fracturing. Fracture spacings have a periodicity of L_m as in Sect. 2.2 above. Equating the flow over the spatially averaged matrix/fracture block of permeability K_{eff} , with the sum of the flow through the matrix (permeability K_m) and the fracture (permeability K_f) yields:

$$K_{eff}L_m = K_mL_m + K_f w_f \quad (10)$$

where we have assumed that $L_m \gg w_f$ (Fig. 1b). Recognising that $K_f \gg K_m$ and inserting Eq. (1), solving for the fracture width w_f gives

$$w_f^3 = 12K_{eff}L_m \quad (11)$$

For example, an extreme but not uncommon value would be those associated with fractured carbonate fields in Oman with primary permeability around $K_m = 10$ mD and a secondary effective permeability estimated at $K_{eff} = 10$ D. Using $L_m = 10$ m then we find typical fracture widths of 1 mm and values of $K_f = 10^5$ D.)

References

- Cheung P, Dubash M, Shen AQ (2012) Local micelle concentration fluctuations in microfluidic flows and its relation to a flow-induced structured phase (FISP). *Soft Matter* 8:2304–2309
- Dogon D, Golombok M (2014) Particle agglomeration in sheared fluids. *J Explor Prod Technol*. doi:10.1007/s13202-014-012102
- Golombok M, van der Wijst R (2012) Permeability thickening fluids for improved secondary oil recovery. *J Petroleum Sci Eng* 110(2013):22–26
- Golombok M, Crane C, Ineke D, Harris J, Welling M (2008) Novel additives to retard permeable flow. *Exp Therm Fluid Sci* 32:1499–1503
- Gonzalez JM, Muller AJ, Torres MF, Eduardo S (2005) The role of shear and elongation in the flow of solutions of semi-flexible polymers through porous media. *Rheol Acta* 44:396–405. doi:10.1007/s00397-004-0421-4
- Hartmann V, Cressely R (1998) Occurrence of shear thickening in aqueous micellar solutions of CTAB with some added organic counterions. *Colloid Polym Sci* 276:169–175
- Moss GR, Rothstein JP (2010) Flow of wormlike micelle solutions through a periodic array of cylinders. *J Non-Newton Fluid Mech* 165:1–13

- Reuvers N, Golombok M (2009a) Parameters for assessing oil reservoir water flooding additives. *ASME J Fluids Eng* 131(1–6):031302
- Reuvers N, Golombok M (2009b) Shear rate and permeability in water flooding. *Transp Porous Med* 79:249–253
- Rojas MR, Müller AJ, Sàez AE (2008a) Synergistic effects in flows of mixtures of wormlike micelles and hydroxyethyl celluloses with or without hydrophobic modifications. *J Colloid Interface Sci* 322(1):65–72
- Rojas MR, Müller AJ, Sàez AE (2008b) Shear rheology and porous media flow of wormlike micelle solutions formed by mixtures of surfactants of opposite charge. *J Colloid Interface Sci* 326(1):221–226
- Rojas MR, Müller AJ, Sàez AE (2010) Effect of ionic environment on the rheology of wormlike micelle solutions of mixtures of surfactants with opposite charge. *J Colloid Interface Sci* 342:103–109
- Turcott D, Schubert G (1982) *Geodynamics: applications of continuum physics to geological problems*. Cornell University Press, Ithaca
- van Golf-Racht TD (1982) *Fundamentals of fractured reservoir engineering*. Elsevier, Amsterdam
- van Heel APG, Boerrigter PM, van Dorp JJ (2008) Thermal and hydraulic matrix-fracture interaction in dual-permeability simulation. *SPE Reserv Evaluat Simul* 11(04):735–749
- Yamamoto T, Hashimoto T, Yamashita A (2008) Flow analysis for wormlike micellar solutions in an axisymmetric capillary channel. *Rheol Acta* 47:963–974